NASA TECHNICAL MEMORANDUM

NASA TM-78158

(NASA-TM-78158) HIGH-RESOLUTION, CONTINUOUS-FLOW ELECTROPHORESIS IN MICROGRAVITY (NASA) 36 p HC A03/MF A01 CSCL 07D

N78-19234

Unclas G3/25 07284

HIGH-RESOLUTION, CONTINUOUS-FLOW ELECTROPHORESIS IN MICROGRAVITY

By Percy H. Rhodes
Space Sciences Laboratory

February 1978

NASA

George C. Marshall Space Flight Center
Marshall Space Flight Center, Alabama

TECHNICAL REPORT STANDARD TITLE PAGE

1. REPORT NO.	2. GOVERNMENT ACCESSION NO.	3. RECIPIENT'S CATALOG NO.
NASA TM-78158		

4. TITLE AND SUBTITLE	5. REPORT DATE
High-Resolution, Continuous-Flow Electrophoresis in Microgravity	February 1978
	6. PERFORMING ORGANIZATION CODE
7. AUTHOR(S)	8. PERFORMING ORGANIZATION REPORT #
Percy H. Rhodes	
9. PERFORMING ORGANIZATION NAME AND ADDRESS	10. WORK UNIT NO.
George C. Marshall Space Flight Center Marshall Space Flight Center, Alabama 35812	11. CONTRACT OR GRANT NO.
	12. TYPE OF REPORT & PERIOD COVERED
12. SPONSORING AGENCY NAME AND ADDRESS	Technical Memorandum
National Aeronautics and Space Administration Washington, D.C. 20546	13. SPONSORING AGENCY CODE

14. SUPPLEMENTARY NOTES

Prepared by Space Sciences Laboratory, Science and Engineering

15. ABSTRACT

Although the possibility of using the reduced gravity of space as a means to enhance the performance of certain electrophoresis devices has been considered for several years, there has been no serious attempt to quantitatively compare electrophoresis performance on the ground with that anticipated in space. The computer mathematical models of various proposed electrophoresis systems that have been devised do not lend themselves to parameter optimization as do analytical expressions. Moreover, there has been no attempt to quantitatively determine the limits imposed on ground-based operation by thermal convection. This report derives approximate expressions which will allow estimation of performance enhancement in reduced gravity and also will direct optimization of the various design parameters for a continuous flow electrophoresis system.

17. KEY WORDS	18. DISTRIBUTION STATEMENT
	Unclassified — Unlimited

19. SECURITY CLASSIF. (of this report)	20. SECURITY CLASSIF. (of this page)	21. NO. OF PAGES	22. PRICE
Unclassified	Unclassified	37	NTIS

TABLE OF CONTENTS

LIST OF ILLUSTRATIONS

TECHNICAL MEMORANDUM 78158

HIGH-RESOLUTION, CONTINUOUS-FLOW ELECTROPHORESIS IN MICROGRAVITY

I. INTRODUCTION

Most biological materials, when dissolved or suspended in a selected aqueous medium, acquire a characteristic electrical charge and will migrate under the influence of an applied field. Separation will, therefore, occur between species of different electrically induced velocity, hence establishing the separation process called electrophoresis.

Separations of biological substances such as living cells must necessarily be conducted in liquid electrolyte of specified properties and, as a consequence, the separation process is compromised by certain gravity-induced distrubances of the media; e.g., sedimentation of the particles and thermal convection of the medium caused by Joule heating. Although various techniques have been developed to overcome these problems on Earth, the elimination of gravity-induced perturbations can be accomplished best in the near-zero-g environment of space.

For several years, the possibility of using the reduced gravity of space has been under consideration as a means to enhance the performance of certain electrophoresis devices. There has, however, been no serious attempt to quantitatively compare electrophoresis performance on the ground with that anticipated in space. Several computer mathematical models of various proposed electrophoresis systems have been devised; however, they do not lend themselves to parameter optimization as analytical expressions do. Moreover, there has been no attempt to quantitatively determine the limits imposed on ground-based operation by thermal convection. This report derives approximate expressions which will allow estimation of performance enhancement in reduced gravity and also will direct optimization of the various design parameters for a continuous flow electrophoresis system.

II. BACKGROUND

Electrophoresis in a free fluid was first demonstrated in space during the Apollo 14 mission [1,2]. This electrophoresis experiment used three materials of different molecular weight: deoxyribonucleic acid (DNA), hemoglobin, and soluble dyes. The separations were photographed periodically during electrophoresis in cylindrical columns. The results showed a separation between the two dyes, and operation of the fluid and electrical systems was normal. The overall results indicated the value of space electrophoresis in microgravity; therefore, plans were made and hardware developed for a subsequent demonstration during the Apollo 16 mission.

The Apollo 16 electrophoresis demonstration was performed using the basic operating elements of the Apollo 14 experiment, but a nonbiological standard sample material, polystyrene latex, was used [1,2]. These stable, nondegradable particles were used as models for living cells. Although a nongravity-related flow perturbation precluded separation of the latex, electrophoresis did occur in the columns containing single species of the latex particles. The photographs clearly show distinct boundaries and sharply defined fronts. The deleterious effects of gravity-induced sedimentation and thermal convection on particle electrophoresis can be seen by comparing the results of the Apollo 16 electrophoresis demonstration with those of ground experiments [2]. These advantages of the space environment for cell separation processes were further confirmed in the demonstration experiment on isotachophoresis of erythrocytes conducted aboard Skylab 4 [3].

The Apollo-Soyuz Test Project (ASTP) [4] electrophoresis experiments separated fixed rabbit, human, and horse red blood cells and also isolated urokinase (UK) producing kidney cells. The process was carried out in static columns similar to those in Apollo 14 and 16. The separation of lymphocytes was also attempted but failed because of a column malfunction. The kidney cell separation was most encouraging, not only because viable cells were carried to orbit, processed, returned, and cultured, but also because the cells which were separated appear to be product specific. That is, from some bands, urokinase appeared to be the prime product the cells produced, while in entirely different bands, human granulocyte conditioning hormone and erythroprotein were the prime products of the cells. This finding is especially important in the case of urokinase when one considers the need for this drug.

While no spectacular results have been achieved from these experiments, it is important to note that the basic premise of space-based electrophoresis — the apparent absence of sedimentation and thermal convection in reduced gravity — was proven in each experiment. It is the purpose of this report to show the significance of the feature of reduced gravity in terms of system performance and also to give equations which might be useful in the development of a device which will take full advantage of reduced gravity.

III. PRINCIPLES OF ELECTROPHORESIS

Contact with a polar (e.g., aqueous) medium produces a surface charge on most substances, the possible charging mechanisms being (a) ionization, (b) ion adsorption, and (c) ion dissolution. The induced surface charge influences the distribution of ions in the surrounding polar medium. While ions of opposite charge (counter-ions) are attracted toward the surface, ions of like charge (co-ions) are repelled away from the surface. An electric double layer [5] is then formed which, aided by the mixing tendency of thermal motion, leads to the configuration of Figure 1. The double layer is then comprised of a charged surface (negative in this case) and a neutralizing excess of counter-ions over co-ions distributed in a diffuse manner in the polar medium.

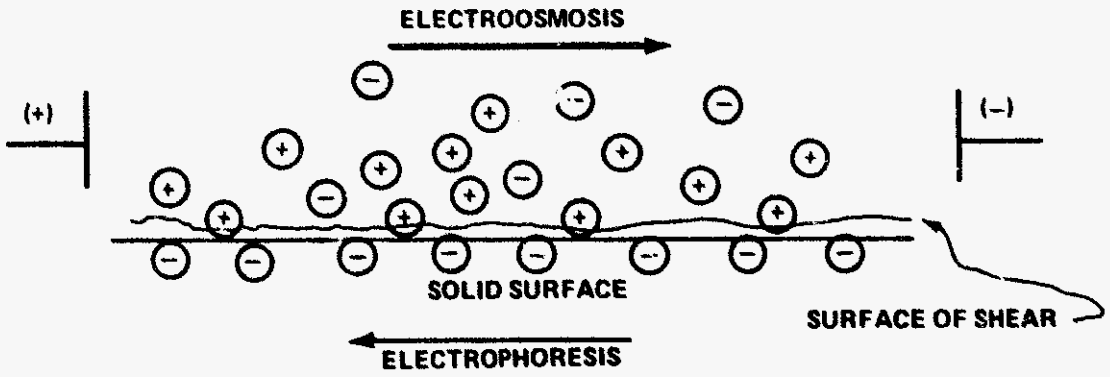

Figure 1. Electric double layer.

Applying an electrical field, as shown, along the charged surface causes a force to be exerted on both parts of the electric double layer. If the charged surface is mobile, it tends to move (together with any attached material) in the

appropriate direction relative to the polar medium. This movement of a particle as a result of its charged surface is called electrophoresis, movement in this case being to the left due to the negative surface charge. Conversely, if the surface is stationary (as with the wall of a separation chamber), movement of counter-ions in the opposite double layer will manifest itself as a net migration carrying along solvent, hence causing fluid flow which is called electroosmosis. The fluid motion involves a slip condition at the surface of shear, causing a fluid layer to move to the right as a result of the excess of counter-ions present. Note that the velocity profile developed by electroosmosis produces velocities in both directions with a plane of zero velocity called the stationary level (Fig. 2). The velocity profile shown in Figure 2 exists in a closed chamber only as a result of continuity and is characterized as "reverse flow."

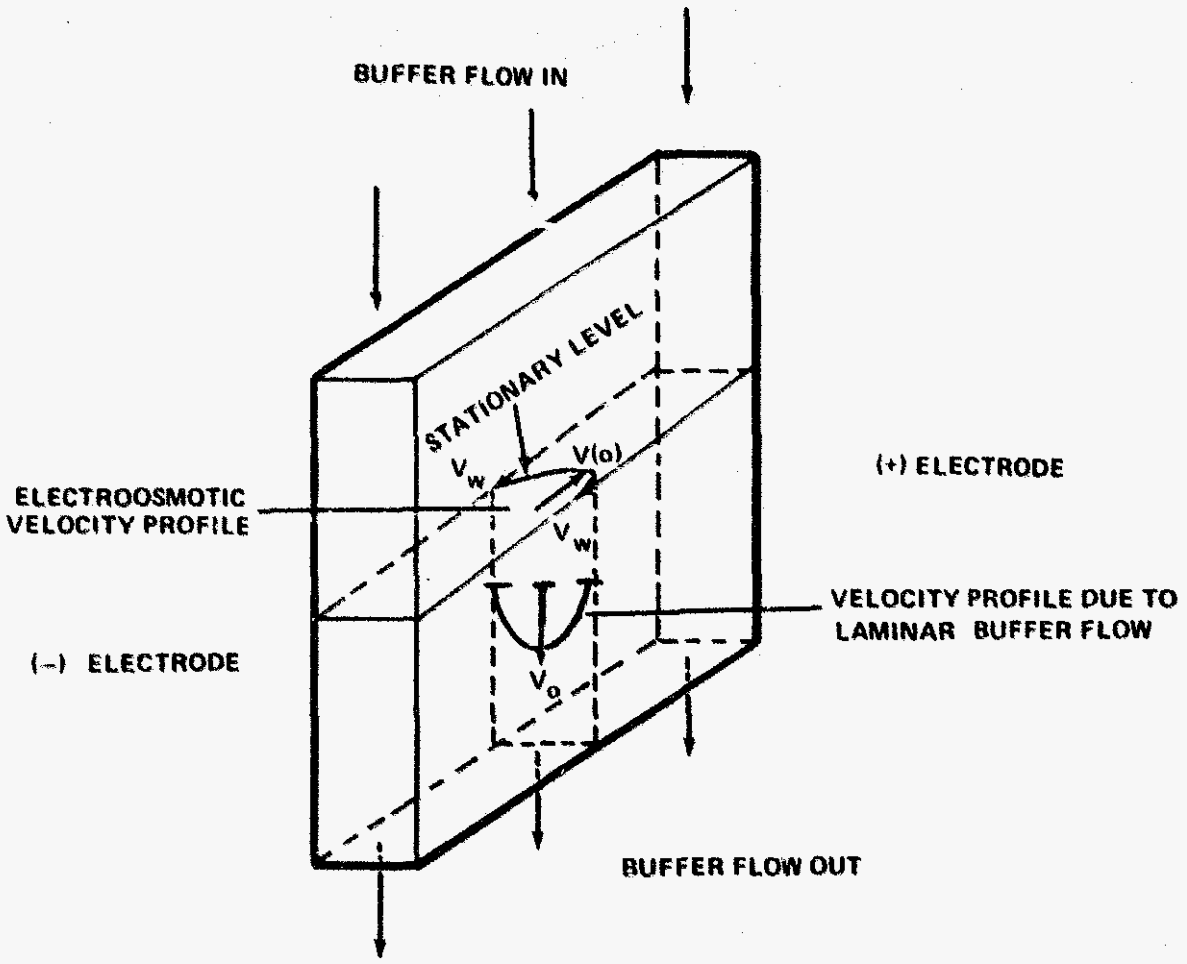

Figure 2. Electroosmotic and laminar flows.

Hence, electroosmosis, being a movement of liquid relative to a stationary charged surface (i.e., a chamber wall) by an applied electrical field, is then the complement of electrophoresis. While electrophoresis is the vehicle for separation and, hence, desirable, electroosmosis can be detrimental or beneficial to system performance depending on the device being utilized.

The electric potential at the surface of shear (slip plane) between the charged surface and the electrolyte solution (buffer) is called the ζ (zeta) potential. The electrophoretic mobility u_e of a particle or dissolved substance is the migration velocity V_e obtained per unit of electrical field gradient E and is related to the zeta potential of the particle, ζ, by the following relations:

$$u_e E = V_e = \frac{\zeta \epsilon}{4\pi\mu} E \qquad (1)$$

where

E = electrical field gradient

ϵ = permittivity

μ = dynamic viscosity.

The previous expression is a steady-state balance between the viscous retarding force and the electrical field force acting on the charged substance in an aqueous medium.

IV. PRINCIPLE OF CONTINUOUS FLOW ELECTROPHORESIS

Continuous flow electrophoresis utilizes a flowing curtain of buffer to provide continuous sample injection and recovery. A sketch of a continuous flow system is shown in Figure 3. The buffer enters at point B and is confined in a thin rectangular chamber while the sample is injected at point A into the downward flowing buffer curtain. Under the influence of a lateral electrical field which impresses a voltage gradient across the width of the chamber, the sample

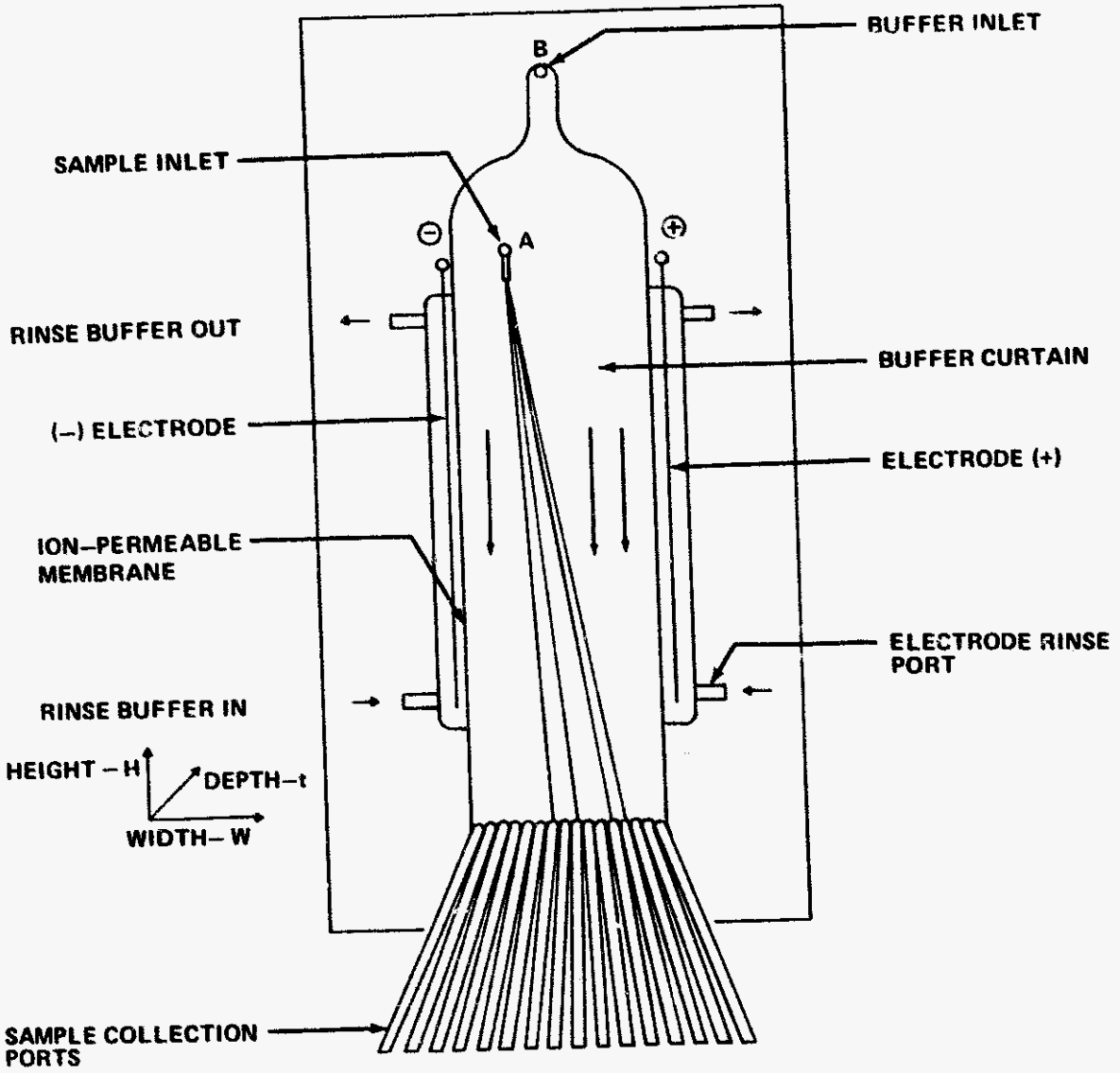

Figure 3. Continuous flow system.

is separated into individual components. The separated sample bands or filaments are continuously fractionated by an array of collection ports situated along the lower width of the chamber. Ion-permeable membranes separate the electrode chamber from the separation chamber.

The ideal resolving power of a continuous flow system can be determined as follows. Consider the separation chamber cross section given in Figure 4a. The ideal distribution of sample is given by equation (1) so that

$$\zeta = \frac{4\pi\mu V_e}{E\epsilon} \quad . \tag{2}$$

Particles along surface 1-1 of the injected sample are distributed according to

$$\zeta_1 = \frac{4\pi\mu y}{E\epsilon\tau}$$

where τ is the residence time. For particles along surface 2-2, sample distribution is

$$\zeta_2 = \frac{4\pi\mu(y - \delta y_1)}{E\epsilon\tau}$$

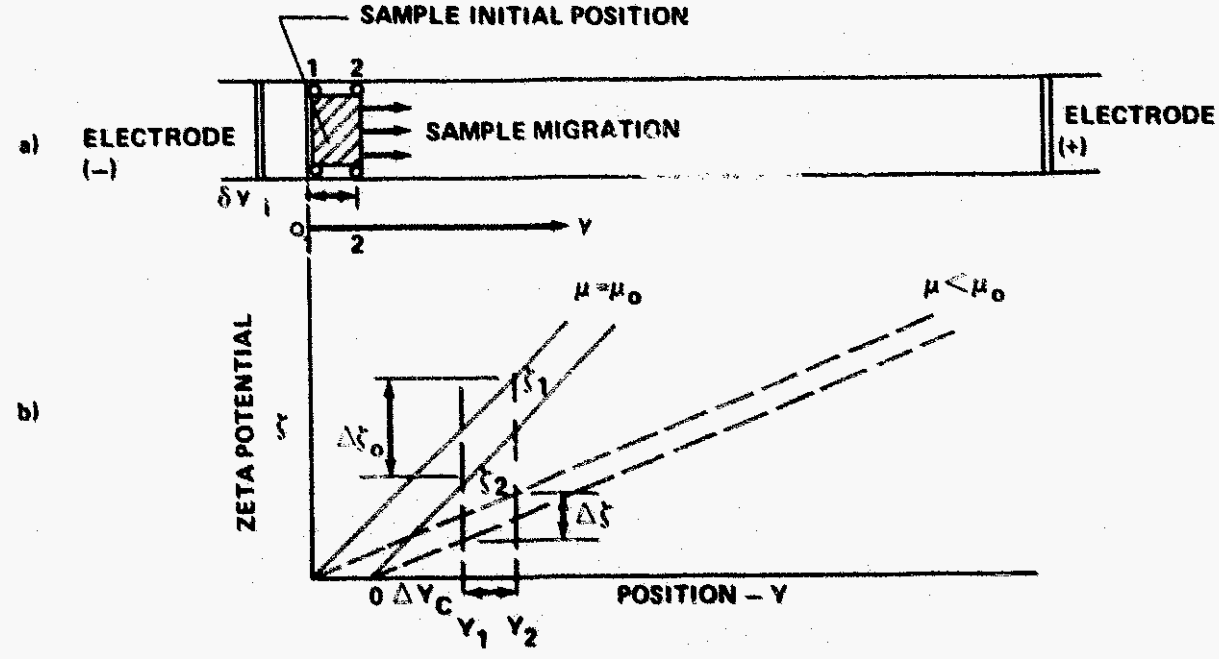

Figure 4. Ideal sample deflection.

where δy_i is the width of the initial sample band. The collection port Y_1-Y_2 collects a distribution width of ΔY_C so that for the fastest particle, ζ_1

$$\zeta_1 = \frac{4\pi\mu Y_2}{E\epsilon\tau} \quad ,$$

since it moves the longest distance, and for the slowest particle

$$\zeta_2 = \frac{4\pi\mu(Y_1 - \delta y_i)}{E\epsilon\tau} \quad .$$

Subtracting gives the resolvable zeta potential difference

$$\Delta\zeta_o = \zeta_1 - \zeta_2 = \frac{4\pi\mu}{E\epsilon\tau}(\Delta Y_C + \delta y_i) \quad . \tag{3}$$

Resolution R is defined as

$$R = \frac{1}{\Delta u} \quad , \tag{4}$$

but u varies with viscosity μ of the buffer which is, in turn, a function of temperature; therefore, we will arbitrarily define mobilities in terms of the viscosity of water at 0°C, so that

$$R = \frac{4\pi\mu^o}{\Delta\zeta\epsilon} \tag{5}$$

where u^o is the viscosity of water at 0°C. Then resolution may be defined in terms of the resolvable zeta potential difference $\Delta\zeta$ which we will call resolution quality. For high resolution we obviously want $\Delta\zeta$ to be small.

It is interesting to note that viscosity μ, field gradient E, and residence time τ in equation (2) combine to enhance resolution quality in reduced gravity. The minimizing of thermal convection in reduced gravity allows the increase in voltage gradient $\underline{E}$ which, in turn, produces a reduction in μ. The residence time τ is limited only by thermal diffusion which must be assessed for each sample of interest, while the field gradient E is limited only by the ability of the biological materials to survive in a heated environment — usually 40°C maximum.

Figure 4b shows graphically how the decrease in μ due to Joule heating of the buffer decreases $\Delta\xi$ collected in the collection port Y_1-Y_2.

V. TEMPERATURE AND VELOCITY DISTRIBUTIONS

The temperature field in the chamber cross section produces a distortion in the injected sample stream. This may be seen by recalling equation (1),

$$u_e(T) = \frac{\xi\varepsilon}{4\pi\mu(T)} \quad ,$$

where it is seen that particles of the same species (i.e., same zeta potential) have different mobilities depending on the local buffer temperature. Joule heating causes the temperature distribution in the chamber cross section, with the maximum temperature occurring at the chamber center plane for equally cooled walls. Obviously, a particle located at the chamber center plane will move farther than a similar particle located nearer the chamber wall, producing what will be termed thermal distortion in this report. In terrestrial operation, thermal convection limits the temperature variation across the thickness of the chamber to values which produce negligible thermal distortion. Thermal distortion, then, is band broadening which is caused by the temperature dependency of buffer viscosity which, in turn, affects the mobility of the sample.

To evaluate separation system performance, it is necessary to determine the temperature distribution in the chamber cross section. Because of the long residence times necessary for high resolution, all heat transfer from the system will be assumed to occur through the chamber walls; hence, the energy equation for a rectangular separation chamber is:

$$\frac{d^2T}{dx^2} = \frac{-Ek_e}{k_t} \tag{6}$$

where

T = buffer temperature in the chamber cross section

x = distance measured away from curtain center plane

E = voltage gradient across width of chamber

k_e = electrical conductivity of buffer

k_t = thermal conductivity of buffer.

The electrical conductivity of the buffer can be approximated by

$$k_e = k_e^o(1 + \alpha T) = \frac{1}{\rho^o}(1 + \alpha T) \tag{7}$$

where

ρ^o = buffer electrical resistivity at 0°C

k_e^o = buffer electrical conductivity at 0°C

α = linear coefficient of electrical conductivity.

Substitution of equation (7) into (6) and solving gives the following temperature distribution:

$$T = \frac{1}{\alpha}\left(\frac{\cos \omega \ell \frac{x}{\ell}}{\cos \omega \ell} - 1\right) \tag{8}$$

where

$$\omega = E \sqrt{\frac{\sigma k_e^o}{k_t^o}}$$

is the dissipation coefficient, ℓ is the chamber half width, and $x/\ell = n$ is the sample-to-chamber thickness ratio. Equation (8) assumes a wall temperature of of 0°C for convenience and to assure maximum operational efficiency. The viscosity expression $\mu(T)$ can be expressed as:

$$\mu(T) = \frac{\mu^o}{1 + \gamma T}$$

$$\mu(n) = \frac{\mu^o}{1 + \frac{\gamma}{\alpha}\left(\frac{\cos \omega \ell n}{\cos \omega \ell} - 1\right)} \qquad (9)$$

where γ is the linear coefficient of viscosity and μ^o is the buffer viscosity at 0°C. The mobility u_e of the particles is thus influenced by the fluid temperature

$$u_e(T) = u_e^o \left[1 + \frac{\gamma}{\alpha}\left(\frac{\cos \omega \ell n}{\cos \omega \ell} - 1\right)\right]$$

$$u_e(T) = u_e^o \left[1 + \frac{\gamma}{\alpha} A(\omega \ell n, \omega \ell)\right] = u_e^o \left[1 + \frac{\gamma}{\alpha} A(n)\right] \qquad (10)$$

where u_e^o is the electrophoretic mobility evaluated at T = 0°C (i.e., at the wall) and

$$A(\omega \ell n, \omega \ell) = \frac{\cos \omega \ell n}{\cos \omega \ell} - 1 = A(n) \quad . \qquad (11)$$

Fluid flow in the chamber is also affected by the viscosity changes with temperature. To obtain the velocity distribution of the sample stream, consider the momentum equation for parallel flow between two flat plates.

$$\frac{\mu^{o}}{1 + \frac{\gamma}{\alpha}\left(\frac{\cos \omega \ell \frac{x}{\ell}}{\cos \omega \ell} - 1\right)} \frac{dV}{dx} = xp_z \qquad (12)$$

where

V = buffer fluid velocity

p_z = pressure gradient along chamber length

x = distance from center plane.

The solution to equation (12) yields:

$$V = V_o D\left(\omega \ell n,\ n,\ \omega \ell,\ \frac{\gamma}{\alpha}\right) = V_o D(n) \qquad (13)$$

where

$$D(n) = \frac{(1 - n^2)\left(\frac{\gamma}{\alpha} - 1\right) + \frac{2\frac{\gamma}{\alpha}}{\omega \ell \cos \omega \ell}\left(\frac{\cos \omega \ell n}{\omega \ell} + n \sin \omega \ell n - \frac{\cos \omega \ell}{\omega \ell} - \sin \omega \ell\right)}{\left(\frac{\gamma}{\alpha} - 1\right) + \frac{2\frac{\gamma}{\alpha}}{\omega \ell \cos \omega \ell}\left(\frac{1}{\omega \ell} - \frac{\cos \omega \ell}{\omega \ell} - \sin \omega \ell\right)} \qquad (14)$$

and V_o is the center plane velocity of buffer relative to chamber wall. Equation (13) yields an elongated parabolic velocity distribution which approaches a parabolic shape as $\gamma/\alpha \rightarrow 0$. The velocity distribution causes particles in the center portion of the chamber to be exposed to the electrical field a shorter length of time (residence time) than particles near the chamber walls. This causes a reversed crescent distortion of the injected sample band as shown in Figure 5. Note that the original sample band CAB is deformed into the crescent shape $\bar{C}\bar{A}\bar{B}$ since particles C and B have longer residence times than particle A. This type of distortion will be identified as flow distortion.

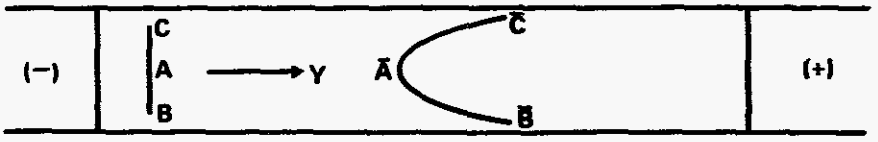

Figure 5. Buffer flow distortion.

Since most materials exhibit a surface charge when placed in contact with an aqueous medium, the charge on the walls of the separation chamber produces electroosmosis under the influence of the applied electrical field. Electroosmosis produces a flow distortion of the sample band which may be used to compensate for the buffer temperature and velocity distortions mentioned previously. The buffer velocity distribution in the chamber cross section (i.e., perpendicular to the buffer flow field) due to electroosmosis can be estimated through the following relationships. The electroosmosis velocity v_{eo} is given by a superposition of parallel flow velocity V(x) with the fluid velocity at the wall; i.e.,

$$v_{eo}(x) = V(x) - v_w \tag{15}$$

where

$v_{eo}(x)$ = the electroosmotic velocity distribution

v_w = the electroosmotic velocity at the wall

$V(x)$ = the parallel fluid velocity between two plates.

The net fluid flow in the cross section must be zero for a closed chamber section. Note that the narrow side walls of the chamber are considered to be closed instead of the chamber ends where buffer must flow into and out of the system, so that

$$Q_{eo} = 2 \int_0^{\ell} [V(x) - v_w] \, dx = 0 \tag{16}$$

where Q_{eo} is net flow in the chamber cross section, perpendicular to the buffer flow, produced by electroosmosis. Using equation (13) and integrating yields

$$v_{eo}(x) = \frac{\frac{3}{2} u_w^o E \left\{ (1-n^2)\left(\frac{\gamma}{\alpha} - 1\right) + \frac{2\frac{\gamma}{\alpha}}{\omega\ell \cos \omega\ell} \left[\frac{\cos \omega\ell n}{\omega\ell} + n \sin \omega\ell - \frac{\cos \omega\ell}{\omega\ell} - \sin \omega\ell \right] \right.}{\left. - u_w^o E \left(\frac{\gamma}{\alpha} - 1\right) + \frac{3\frac{\gamma}{\alpha}}{\omega\ell \cos \omega\ell} \left[\frac{2 \sin \omega\ell}{(\omega\ell)^2} - \frac{2 \cos \omega\ell}{\omega\ell} - \sin \omega\ell \right] \right.} \tag{17}$$

where u_w^o is the electroosmotic mobility at the wall which is at 0°C. The preceding buffer temperature and velocity distributions affect the shape of the injected sample bands which, in turn, affect the system performance. This is due to the fact that the sample collection ports are usually circular or rectangular in shape and are necessarily arranged regularly along the lower width of the separation chamber. Sample band distortion or apparent band broadening, however, causes species to be collected over many collection ports, resulting in remixing and a degradation in resolution. A regular or narrow band will, however, be collected in only a few ports, resulting in high resolution. Therefore, minimization of sample band distortion, as well as increased voltage gradients and longer residence times as mentioned previously, is of primary importance in high resolution electrophoresis.

VI. CONTINUOUS FLOW ELECTROPHORESIS PERFORMANCE

The electrophoretic migration velocity v_e is given by

$$v_e = \frac{\zeta \epsilon}{4\pi\mu} E \quad ,$$

so that substituting for μ in equation (10) and using

$$u_e^o = \frac{\zeta \epsilon}{4\pi \mu^o} \quad ,$$

we obtain

$$v_e = u_e^o E \left[1 + \frac{\lambda}{\alpha}\left(\frac{\cos \omega t n}{\cos \omega t} - 1\right)\right] \tag{18}$$

where μ^o is the buffer viscosity at 0°C. The local residence time, $\tau(n)$, for any particle is given by

$$\tau(n) = \frac{H}{V(n)} = \frac{H}{V_o D} \tag{19}$$

where H is the electrode length, D is given by equation (14), and V is the local buffer velocity. The particle migration velocity is given by the sum of the electrophoretic migration velocity and the electroosmotic fluid velocity in the chamber cross section, so that the displacement Y becomes

$$Y = \tau_o \left[v_e + V_{eo}\right] = \frac{H}{v_o D} \left[v_e + v_{eo}\right] \tag{20}$$

or

$$Y = \frac{EH}{V_o} u_e^o \frac{\left[1 - \frac{u_w^o}{u_e^o} + \frac{\gamma}{\alpha} A(n)\right]}{D(n)} + \frac{3}{2} u_w^o B\left(\omega\ell, \frac{\gamma}{\alpha}\right) \tag{21}$$

where

$$B\left(\omega\ell, \frac{\gamma}{\alpha}\right) = \frac{\omega\ell \cos \omega\ell \left(1 - \frac{\alpha}{\gamma}\right) + 2\left[\frac{1}{\omega\ell} - \frac{\cos \omega\ell}{\omega\ell} - \sin \omega\ell\right]}{\omega\ell \cos \omega\ell \left(1 - \frac{\alpha}{\gamma}\right) + 3\left[2 \frac{\sin \omega\ell}{(\omega\ell)^2} - 2 \frac{\cos \omega\ell}{\omega\ell} - \sin \omega\ell\right]} \tag{22}$$

Equation (21) is a general expression for particle displacement in a continuous flow electrophoresis device. Figure 6 shows the sample band distortion in a continuous flow system.

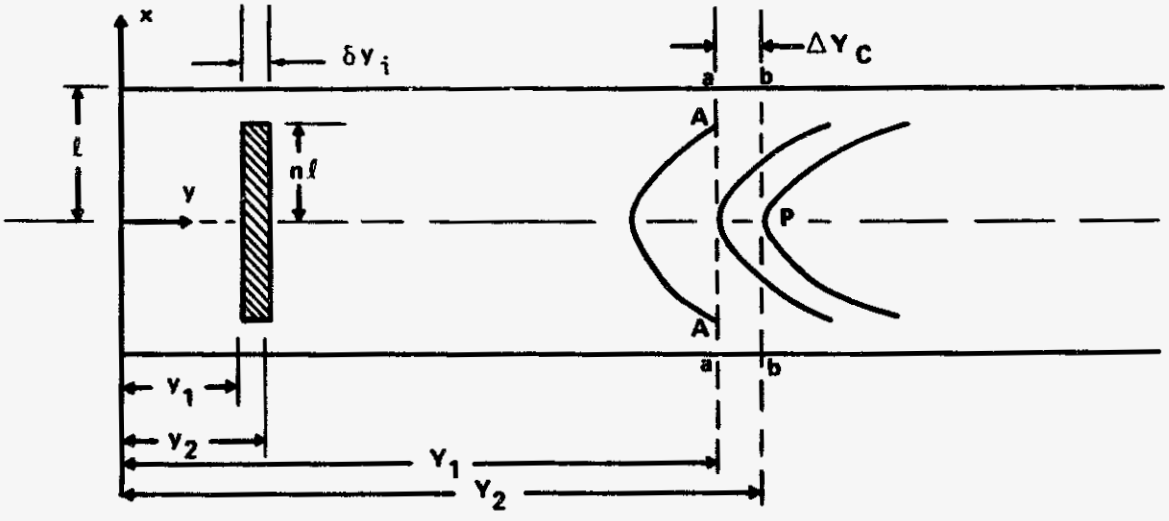

Figure 6. Sample band distortion in a continuous flow system.

To determine the resolvable mobility difference Δu^o, the highest and lowest mobility particles entering a typical collection port must be found. The initial sample width is δy_i, while ΔY_C is the width of the collection port. The fastest particle entering the port will do so at point P and must travel the farthest distance of all particles entering the port. Therefore, migration equation for the fastest particle u_2^o is given by

$$Y_2 - Y_1 = \frac{E\tau u_2^o \left[1 - \frac{u_w^o}{u_2^o} + \frac{\gamma}{\alpha} A(n)\right]}{D(n)} + \frac{3}{2} u_w^o B\left(\omega\ell, \frac{\alpha}{\gamma}\right) \Bigg| \begin{array}{l} \text{Point P,} \\ n = 0 \end{array} \qquad (23a)$$

while that for the slowest particle u_1^o entering the port is given by

$$Y_1 - Y_2 = \frac{E\tau u_1^o \left[1 - \frac{u_w^o}{u_1^o} + \frac{\gamma}{\alpha} A(n)\right]}{D(n)} + \frac{3}{2} u_w^o B\left(\omega\ell, \frac{\alpha}{\gamma}\right) \Bigg| \text{ Point A} \qquad (23b)$$

where $\tau = H/V_o$ is the nominal residence time, i.e., the residence time for a particle on the center plane, and the superscript o denotes property evaluation 0°C. Subtracting equations (23a) and (23b) and substituting ΔY_C and δy_i yields an estimate for resolvable mobility difference Δu^o for the backward-shaped crescent shown:

$$\Delta u^o \left[1 + \frac{\gamma}{\alpha} A(o)\right] = \frac{\Delta Y_C + \delta y_i}{E\tau} + (u_1^o - u_w^o)\left[\frac{1 - D(n)}{D(n)}\right]$$

$$+ u_1^o \frac{\gamma}{\alpha}\left[\frac{A(n)}{D(n)} - A(o)\right] \quad . \qquad (24)$$

A similar analysis for the forward-shaped crescent deformation yields

$$\Delta u^o \left[1 + \frac{\gamma}{\alpha} A(o)\right] = \frac{\Delta Y_C + \delta y_i}{E\tau} + (u_w^o - u_2^o)\left[\frac{1 - D(n)}{D(n)}\right] + u_2^o \frac{\gamma}{\alpha}\left[A(o) - \frac{A(n)}{D(n)}\right] \quad . \tag{25}$$

Equations (24) and (25) can be combined into a general expression for resolvable mobility difference Δu^o for cases of high resolution where $u_2^o \approx u_1^o = u_e^o$:

$$\Delta u^o \left[1 + \frac{\gamma}{\alpha} A(o)\right] = \frac{\Delta Y_C + \delta y_i}{E\tau} + \left| (u_w^o - u_e^o)\left[\frac{1 - D(n)}{D(n)}\right] + u_e^o \frac{\gamma}{\alpha}\left[A(o) - \frac{A(n)}{D(n)}\right] \right| \tag{26}$$

The resolvable mobility difference Δu^o can be reduced to resolution quality $\Delta\zeta$ through equation (2):

$$\Delta\zeta \left[1 + \frac{\gamma}{\alpha} A(o)\right] = \frac{4\pi\mu^o}{\epsilon}\left\{\frac{(\Delta Y_C + \delta y_i)\,\ell}{k_p^o(\omega\ell)\tau} + \left| (\zeta_w - \zeta_e)\frac{1 + D(n)}{D(n)} + \zeta_e \frac{\gamma}{\alpha}\left[A(o) - \frac{A(n)}{D(n)}\right] \right|\right\} \tag{27}$$

where k_p^o is a buffer property constant

$$k_p^o = \sqrt{\frac{Kk_t^o\rho^o}{\alpha}}$$

so that

$$E = k_p^o \omega$$

and

$$\alpha = 0.04/^\circ C$$

$$k_t = 1.36 \times 10^{-3} \text{ cal/sec cm } ^\circ C$$

$$\rho^o = 1.93 \times 10^3 \ \Omega \text{ cm}$$

$$K = 4.148 \text{ W sec/cal.}$$

Equation (27) defines the resolution capability of a continuous flow device. The terms in the equation have the following significance: $[1 + \gamma/\alpha \ A(o)]$ gives the increase in resolution due to the decreased viscosity caused by Joule heating as discussed previously in Section IV, while $(\Delta Y_C + \delta y_i) \ell / k_p^o (\omega \ell) \tau$ is the ideal resolving power of the device (i.e., the resolving power neglecting distortion effects), and

$$\left| (\zeta_w - \zeta_e) \frac{[1 + D(n)]}{D(n)} + \zeta_e \frac{\partial}{\partial \alpha} \left[A(o) - \frac{A(n)}{D(n)} \right] \right|$$

gives the effect on resolution of flow and thermal distortion. Note that this term can be minimized by proper selection of the wall zeta potential and low ζ_e.

VII. ELECTROPHORESIS PERFORMANCE LIMITATION IN EARTH GRAVITY

The foregoing estimate of continuous flow electrophoresis performance is valid for space environments in which the effects of thermal convection have been shown to be negligible. It is also valid, however, for terrestrial operation

in which the chamber power dissipation is below the threshold where convective disturbance is discernible in regard to separation performance.

The onset of convective disturbances may be correlated with chamber power input and buffer flow velocity. It is well known that high buffer flow velocities stabilize against thermal convection. This leads one to suspect that there could be a relation between convection-induced velocity and buffer flow velocity which delineates the onset of perceivable disturbances to the separation process.

An investigation conducted by the General Electric Company under NASA Contract NAS8-31036 [6] determined experimentally the effect of residence time on the maximum usable power. The input power was increased gradually on a $0.5 \times 10 \times 5$ cm test chamber operating at various buffer flow rates until visible sample stream perturbations were observed. The results of these investigations are given in Figure 7. Note that a horizontally inclined chamber gave the higher usable power levels; however, these results will not be considered here since sedimentation is not controlled in the horizontal orientations. It is important to note that very little difference in acceptable power input is observed between the 0° and 180° orientations. Therefore, using the conventional downward flowing buffer (0° orientation), estimates can be calculated for the convection-induced velocities using the following equation (Appendix):

$$u_C = \omega \ell \sqrt{\frac{\beta g \ell}{2\alpha}} \tag{28}$$

where

u_C = convection induced velocity (cm/sec)

β = coefficient of thermal expansion (1/°C)

g = gravitational constant

ℓ = chamber half thickness (cm)

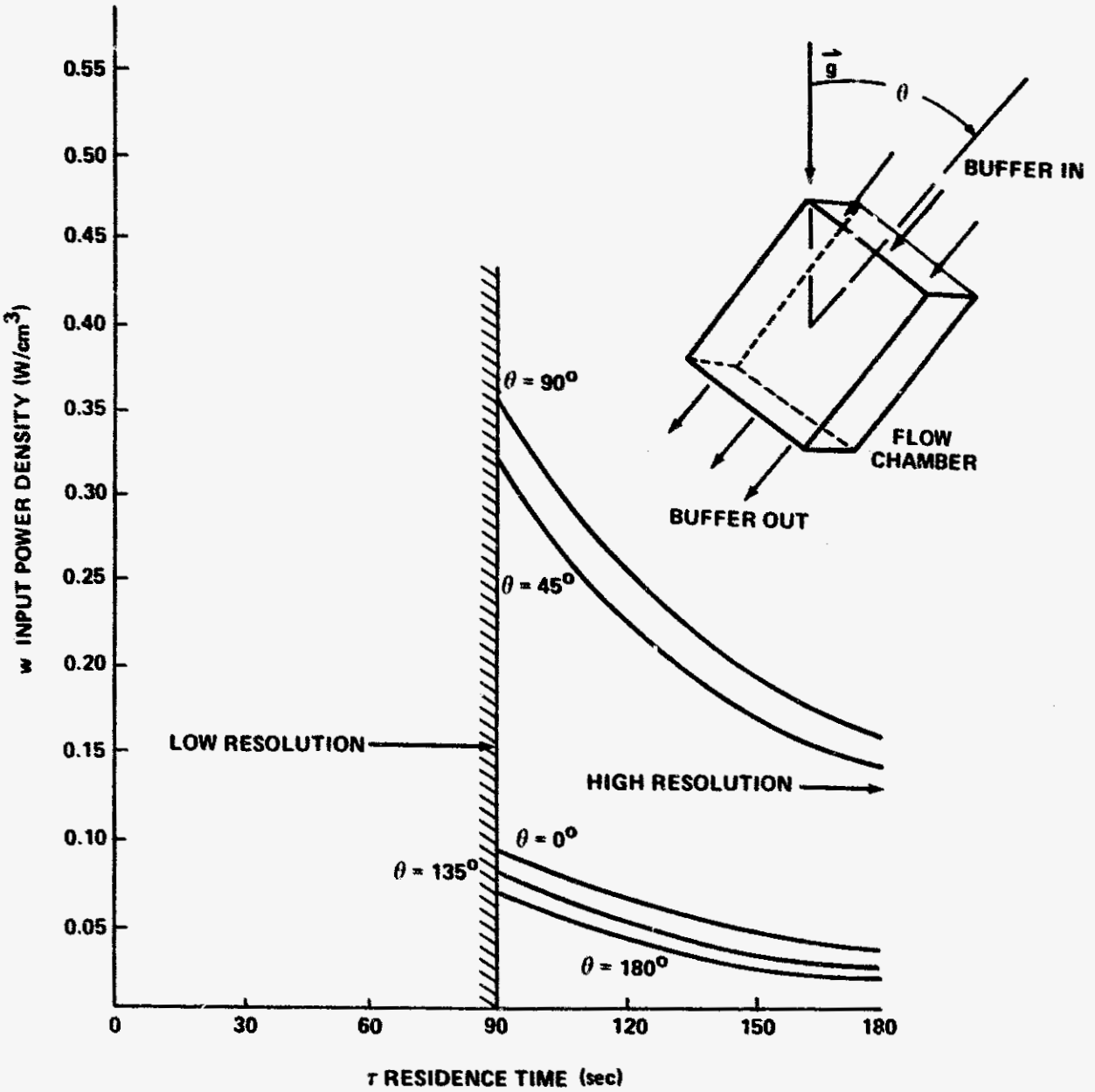

Figure 7. Onset of convective disturbances.

A comparison of convection-induced velocity to chamber midplane velocity for the 0.5 cm chamber is given in Table 1. These results suggest the following

TABLE 1. COMPARISON OF BUFFER AND CONVECTION VELOCITIES

τ (sec)	w (W/cm^3)	$\omega\ell$	V_o (cm/sec)	u_C (cm/sec)
180	0.04	0.14	0.06	0.10
150	0.04	0.14	0.07	0.10
120	0.055	0.16	0.08	0.12
90	0.080	0.19	0.11	0.14

relation between convection-induced velocity and buffer flow velocity at the threshold of perceivable convective disturbances in a continuous flow system:

$$u_C = 0.29\ V_o^{1/3} \tag{29}$$

and

$$\omega\ell \sqrt{\frac{\beta g \ell}{2\alpha}} = 0.29\ V_o^{1/3}$$

so that the maximum dissipation number $\overline{\omega\ell}$ is given by

$$\overline{\omega\ell} = 0.29\ V_o^{1/3} \sqrt{\frac{2\alpha}{\beta g \ell}} = 0.29 \left(\frac{H}{\tau}\right)^{1/3} \sqrt{\frac{2\alpha}{\beta g \ell}} \quad , \tag{30}$$

where

$\alpha = 1/°C$

$H = cm$

$\tau = sec$

$\beta = 0.18 \times 10^{-3}/°C$

$\ell = cm.$

The expression for $\overline{\omega\ell}$ in equation (30) is admittedly based on rather sketchy data for only a 0.5 cm chamber; however, the limitation of operation of a Beckman CPE located at General Electric's Space Sciences Laboratory has been observed to be

$\tau = 200$ sec

$E = 100$ V/cm

where

$H = 60$ cm

$\ell = 0.075$ cm.

Equation (30) predicts that the threshold of convectional perturbations will be

$\overline{\omega\ell} = 0.48$

$E = 105$ V/cm.

Thus, a significant degree of correlation is shown for a different sized chamber. It is important to note that equation (30) limits the usable voltage gradient in Earth gravity as a function of the residence time.

VIII. INPUT POWER LIMITATIONS IN REDUCED GRAVITY

Having assessed the operational limitations of Earth-based, continuous-flow electrophoresis, we now determine those limitations present in a space environment. The limit imposed on the usable voltage gradient in reduced gravity is determined by the temperature sensivity of the sample being separated. Although each sample would certainly vary, a value of 30°C at the chamber mid-plane is commonly accepted as a nominal safe temperature. Thus, the maximum dissipation number in reduced gravity is given by equation (8) as

$$\overline{\omega\ell} = \cos^{-1}\left(\frac{1}{1 + T\alpha}\right) \tag{31}$$

$$\overline{\omega\ell}_{space} = 1.10 \quad .$$

IX. RESIDENCE TIME LIMITATION IN REDUCED GRAVITY

If 1×10^{-4} g is considered to be the nominal gravitational attraction in reduced gravity, then equation (30) shows that the permissible residence time for a normal-sized chamber is not limited by thermal convection. The other potential constraint on residence time would be diffusion, which would not be affected by the reduction of gravity. Considering first particles such as cells whose mean diameter is $> 1\mu$, we obtain a diffusion coefficient of $D = 4.5 \times 10^{-9}$ cm^2/sec. The root-mean-square lateral displacement of particles caused by diffusion is given by the Einstein relationship

$$\bar{\Delta x} = (2\,D\tau)^{1/2} \quad . \tag{32}$$

Then, where

$$\tau = 900 \text{ sec}$$

we have

$$\overline{\Delta x} = 0.0028 \text{ cm} = 28\,\mu$$

which is insignificant with regard to resolution. However, proteins have a much higher diffusion coefficient which would limit the allowable residence time τ. Using $D = 6.0 \times 10^{-7}$ cm^2/sec as a representative diffusion coefficient for proteins, we have for $\tau = 500$ sec a significant displacement of the band edges

$$\overline{\Delta x} = 0.0245 \text{ cm} \quad .$$

Diffusion broadening causes the band width to broaden by

$$B_w = 2\,\overline{Dx}$$

since the perimeter of the stream cross section is displaced. Band thickening in the chamber cross section is, therefore, also given by

$$B_t = 2\,\overline{Dx} \quad .$$

and with distortion present there results a much larger degradation in resolution than the linear effect of width broadening. Therefore, in protein separation, a definite limit in residence time does exist and is governed mainly by the flow and thermal distortions present. The effect of diffusion on resolution can be estimated by modifying equation (27):

$$\overline{\Delta u}^{o}\left[1 + \frac{\gamma}{\alpha} A(o)\right] = \frac{\Delta Y_C + 2\,\overline{Dx} + \delta y_i}{E\tau} + u_e \left| \left(\frac{u_w}{u_e} - 1\right) \frac{1 - D(n)}{D(n)} + \frac{\gamma}{\alpha}\left[A(o) - \frac{A(n)}{D(n)}\right] \right| . \tag{33}$$

The linear effect of band widening is reflected in the first right-side term, while the effect of band thickening (i.e., an increase in n) is reflected in the distortion term (the second right-side term).

X. EFFECT OF BAND DISTORTION ON RESOLUTION

The fact that the collection ports are regular in cross section and arrangement dictates that the injected sample filaments remain regular and undistorted in the chamber cross section. The effect of sample filament distortion on resolution can be estimated by the term:

$$R_d = u_e^o \left| \left(\frac{u_w^o}{u_e^o} - 1\right) \frac{1 - D(n)}{D(n)} + \frac{\gamma}{\alpha}\left[A(o) - \frac{A(n)}{D(n)}\right] \right| \tag{34}$$

where R_d is the residual due to flow and thermal distortion. At the chamber midplane $n = 0$ so that $R_d = 0$, but at other values of n, R_d depends on u_w^o / u_e^o, u_e^o, and γ / α. The term u_w^o / u_e^o may be adjusted to provide $R_d = 0$ for a particular n, but there is no position in the chamber width where $R_d = 0$ throughout the chamber depth as approached when thermal effects are small. Neglecting thermal effects in Earth gravity is permissible because of the low power inputs allowed; however, in reduced gravity where high power inputs are feasible, the residual R_d must be minimized by careful selection of design and operating parameters. Adjusting the buffer to provide a low u_e^o would be one method to control sample filament distortion.

XI. COMPARISON OF RESOLUTION FOR TERRESTRIAL AND REDUCED GRAVITY OPERATION

To estimate the improvement in resolution that might be obtained by operating in reduced gravity, consider the following hypothetical separation:

$$u_e^o = 0.1\ \mu\ \text{cm/V sec}^1$$

$$\frac{\gamma}{\alpha} = 1.0$$

$$n = 0.5$$

$$\tau_S = 800\ \text{sec}$$

$$\tau_G = 200\ \text{sec}$$

$$\ell_S = 0.1\ \text{cm},\ 0.25\ \text{cm}$$

$$\ell_G = 0.1\ \text{cm}$$

$$(\omega\ell)_G = 0.48$$

$$(\omega\ell)_S = 1.10$$

where subscripts S and G stand for space and ground, respectively. Equation (26) and the previous hypothetical parameters were used to produce the performance curves shown in Figure 8.

---

1. The low mobility must be obtained through utilization of an appropriate buffer.

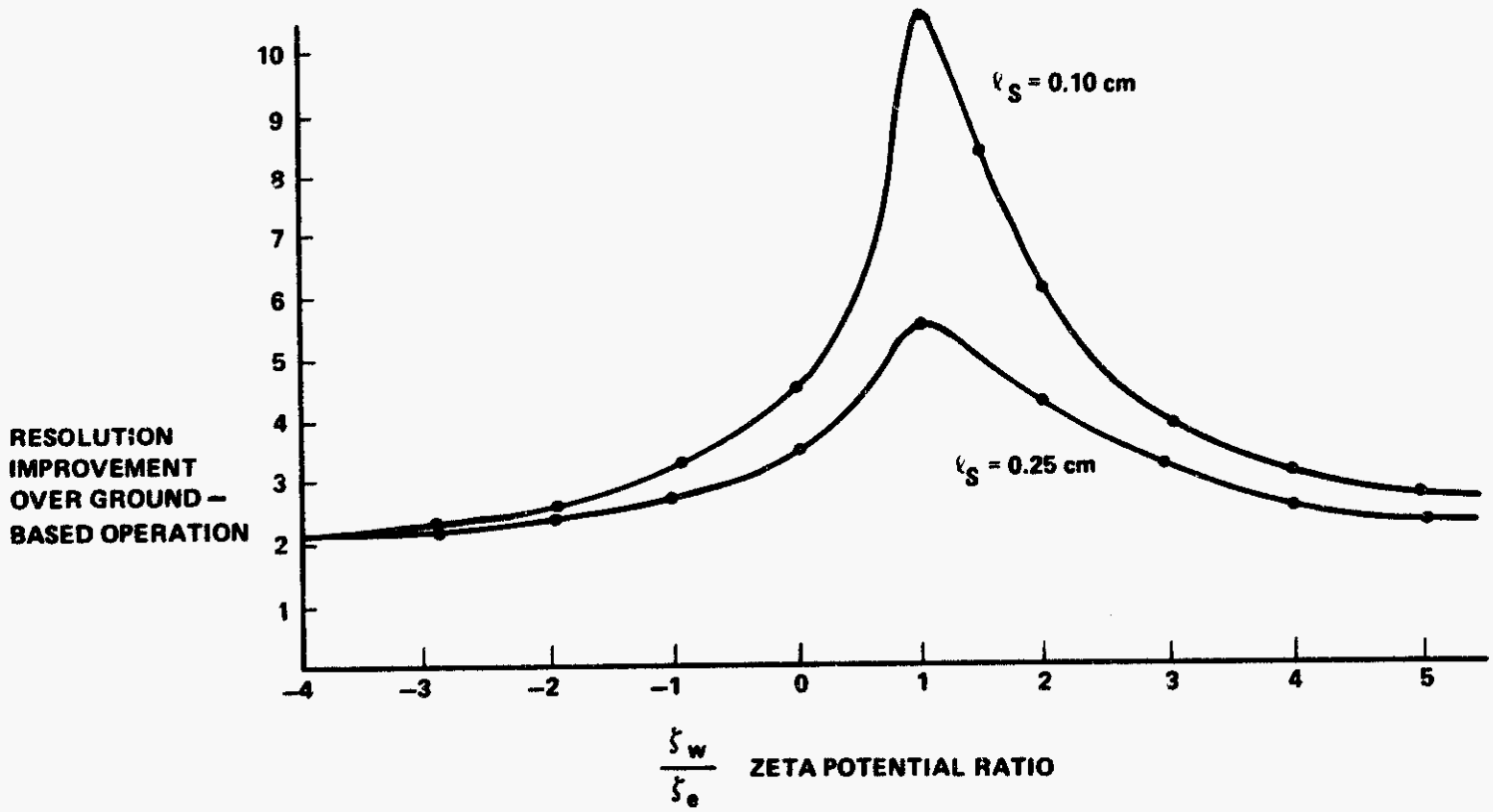

Figure 8. Comparison of space versus ground resolution.

Figure 8 clearly shows that sample band distortion can significantly reduce resolution improvement. Therefore, a close matching of wall and particle zeta potentials must be maintained for space-based high-resolution electrophoresis. Note also that the thin chamber is affected much more by the zeta potential mismatch than the thick chamber, but it also has a much higher resolution potential.

XII. DESIGN CONSIDERATIONS FOR HIGH RESOLUTION ELECTROPHORESIS IN SPACE

The absence of the thermal convection influence allows higher voltage gradients and longer residence times to be used. While this increases resolution, it also increases the particle deflection to such an extent that impractical chamber widths are necessary. Since high particle mobilities also increase thermal distortion, as equation (34) indicates, it is necessary to limit the particle mobility of interest by controlling the pH of the buffer accordingly. Research is in progress at the Marshall Space Flight Center to determine isoelectric points of various potential sample materials. Of course, typical isoelectric points with regard to biological function considerations would be of critical importance to the concept of high resolution electrophoresis in space.

Consider the following example: chamber width $W = 2$ cm, residence time $\tau = 800$ sec, voltage gradient $E = 180$ V/cm, and u_m = maximum mobility of interest. These values would result in

$$u_m = \frac{W}{E\tau} = 0.14 \times 10^{-4} \frac{cm^2}{V\ sec} = 0.14 \frac{\mu\ cm}{V\ sec} \quad .$$

Therefore, we must approach the isoelectric point of the fractions of interest to collect them since all other fractions will be wasted by migration into the chamber end boundaries. Therefore, the selection of a particular fraction to be collected will, in turn, be made by buffer pH selection.

The concept of a "thick" chamber has been proposed for use in reduced gravity to achieve increased throughput and higher resolution. The increase in resolution would be achieved by keeping the sample away from the chamber walls

via the increased chamber thickness, and hence reduce sample band distortion. Equation (27), however, shows that the distortion term contains $\omega\ell$, n, and γ/α, and not ℓ. On the contrary, the resolution is seen to decrease with increasing ℓ for constant power dissipation number $\omega\ell$. This results because the increase in thickness will also dictate a lower voltage gradient E for constant midplane temperature, therefore, resolution suffers. The throughput, indeed, increases with chamber thickness, as is obvious in Figure 8 which shows that a thick chamber produces very nearly the same resolution at a ζ_w^o/ζ_e^o of ±5 as a thin chamber does while giving four times the throughput. Therefore, when a high degree of band distortion is allowable (i.e., low resolution applications), the thick chamber is superior. Another characteristic of the "thick" chamber configuration is less power consumption for equal chamber volumes. Because power dissipated in the chamber varies as the square of the voltage gradient and only linearly with thickness, a "thin" chamber can dissipate more power than a "thick" one without exceeding a limiting centerplane temperature. However, using a "thick" chamber to allow lower voltage gradients is hardly tenable from a resolution standpoint since utilization of high-voltage gradients is a significant reason for reduced gravity operation. Moreover, "thin" chambers are more stable against perturbations than "thick" chambers, as the appropriate dimensionless ratios of viscous to disturbing forces indicate.

XIII. CONCLUSIONS

Cell separation in reduced gravity by continuous flow electrophoresis is feasible, and significant gains in resolution over ground-based operation are possible. The higher voltage gradients and longer residence times available in space operation are responsible for these gains. The mobility of the fraction of interest, however, must be reduced by an order of magnitude from that normally found in terrestrial separations. The higher voltage gradients and longer residence times dictate this reduction in mobility to keep the particle displacements within reasonable limits.

APPENDIX

An estimate of convection-induced velocity is given by

$$u_C = \sqrt{\beta g \Delta T \ell} \qquad \text{for } Gr \geq 1$$

where ΔT is the temperature rise in the chamber cross section over the wall temperature and is given by

$$\Delta T = \frac{4E^2\ell^2}{8Kk_t\rho}$$

assuming constant buffer properties.[1] Therefore, the convection-induced velocity becomes

$$u_C = \sqrt{\frac{\beta g E^2 \ell^2}{2Kk_t\rho}\ell} \quad ,$$

but the power dissipation coefficient ω is

$$\omega = \frac{E}{k_p^o} = E\sqrt{\frac{\alpha}{\rho k_t K}}$$

or

$$E^2 = \frac{Kk_t\rho}{\alpha}\omega^2$$

so that

$$u_C = \sqrt{\frac{\beta g \omega^2 \ell^2 \ell}{2\alpha}} = \omega\ell\sqrt{\frac{\beta g \ell}{2\alpha}} \quad .$$

---

1. Ground-based operation is limited to power dissipations for which this assumption is valid.

REFERENCES

1. McKannan, E. C., Krupnick, A. C., Griffin, R. N., and McCreight, L. R.: Electrophoresis Separation in Space — Apollo 14. NASA TM X-64611, 1971.

2. Snyder, R. S., Bier, M., Griffin, R. N., Johnson, A. J., Leidheiser, H., Micale, F. J., Ross, S., and van Oss, C. J.: Free Fluid Particle Electrophoresis on Apollo 16. Separation and Purification Methods, vol. 2, 1973, pp. 259-282.

3. Bier, M., Hinckley, J. O. N., and Smolka, A. J. K.: Potential Use of Isotachophoresis in Space. Protides of the Biological Fluids, 22nd Colloquim, H. Peeters (ed.), Pergamon Press, New York, 1975, pp. 673-678.

4. Allen, R. E., Barlow, G. H., Bier, M., Bigazzi, P. E., Knox, R. J., Micale, F. J., Seaman, G. V. F., Vanderhoff, J. W., van Oss, C. J., Patterson, W. J., Scott, F. E., Rhodes, P. H., Nerren, B. H., and Harwell, R. J.: Electrophoresis Technology Experiment MA-011. NASA TM X-58173, 1976, pp. 20-1 — 20-23.

5. Shaw, D. J.: Electrophoresis. Academic Press, New York, 1969.

6. Semon, Howard W.: Investigation of Flow Stability in the SPAR Wide-Gap Electrophoretic Separation Chamber. Contract NAS8-31036, General Electric Company, Philadelphia, Pennsylvania, July 15, 1977.

APPROVAL

HIGH-RESOLUTION, CONTINUOUS-FLOW ELECTROPHORESIS IN MICROGRAVITY

By Percy H. Rhodes

The information in this report has been reviewed for security classification. Review of any information concerning Department of Defense or nuclear energy activities or programs has been made by the MSFC Security Classification Officer. This report, in its entirety, has been determined to be unclassified.

ROBERT S. SNYDER
Chief, Separation Processes Branch

ROBERT J. NAUMANN
Chief, Space Processing Division

CHARLES A. LUNDQUIST
Director, Space Sciences Laboratory

U. S. GOVERNMENT PRINTING OFFICE 1978 - 740 193/259 REGION NO. 4